Generalized dynamical thermostating technique

Brian B. Laird
Department of Chemistry and Kansas Institute for Theoretical and Computational Science, University of Kansas, Lawrence, Kansas 66045, USA

Benedict J. Leimkuhler
Department of Mathematics and Computer Science, University of Leicester, Leicester LE1 7RH, United Kingdom
(Received 2 April 2003; published 29 July 2003)

We demonstrate that the Nosé method for constant-temperature molecular-dynamics simulation [Mol. Phys. **52**, 255 (1984)] can be substantially generalized by the addition of auxiliary variables to encompass an infinite variety of Hamiltonian thermostats. Such thermostats can be used to enhance ergodicity in systems, such as the one-dimensional harmonic oscillator or certain molecular systems, for which the standard Nosé-Hoover methods fail to reproduce converged canonical distributions. In this respect the method is similar in spirit to the method of Nosé-Hoover chains, but is both more general and Hamiltonian in structure (which allows for the use of efficient symplectic integration schemes). In particular, we show that, within the generalized Nosé formalism outlined herein, any Hamiltonian system can be thermostated with any other, including a copy of itself. This gives one an enormous flexibility in choosing the form of the thermostating bath. Numerical experiments are included in which a harmonic oscillator is thermostated with a collection of noninteracting harmonic oscillators as well as by a soft billiard system.

DOI: 10.1103/PhysRevE.68.016704 PACS number(s): 02.70.Ns, 05.20.Gg, 05.45.Pq, 87.15.Aa

I. INTRODUCTION

The use of extended dynamical systems to generate trajectories with phase points distributed according to a canonical (isothermal) distribution, as opposed to the microcanonical (isoenergetic) distribution generated by traditional Hamiltonian dynamics, has become standard in molecular-dynamics simulation. Of the available approaches, those based on the extended Hamiltonian of Nosé are the most widely used. In this method, the Hamiltonian of the system is augmented by the addition of auxiliary dynamical variables, so that constant-energy dynamics in the extended phase space generates a canonical distribution in the reduced phase space of the original system, assuming ergodicity. Although this method is popular, it exhibits limitations when applied to large scale systems with complex chemical structure, such as protein-bath models and quantum-classical systems for which a variety of dynamical components are present in the solution. These limitations are a direct result of the simplicity of the Nosé method (which is also one of its most desirable features) and they are only partly ameliorated by the introduction of various devices such as Nosé chains. In this paper, we show how Nosé's approach can be generalized to incorporate a wide range of bath systems, offering many interesting avenues for improved dynamic sampling. We also demonstrate the construction of efficient numerical methods for this system.

Following the original papers of Nosé [1,2], many modifications of the basic formulation have been proposed. Nosé dynamics accomplishes thermostating by a dynamic (and artificial) modification of the time scale. In Ref. [3], time and coordinate transformations are introduced to correct the time-scale problem; the resulting Nosé-Hoover dynamics is non-Hamiltonian, although a conserved energy function does exist. The lack of Hamiltonian structure precludes the use of symplectic numerical integration schemes, which have been shown to yield superior long term stability [3], and the design of algorithms for this system has focused on the development of time-reversible methods [4]. In an alternative approach [5,6], a Poincaré time transformation is applied to the Nosé Hamiltonian, yielding a new Hamiltonian, which generates canonically distributed dynamics directly in real time. Although the exact phase-space trajectories for the Nosé-Hoover and Nosé-Poincaré methods can easily be shown to be identical, the Nosé-Poincaré dynamics is Hamiltonian, allowing for the design of *symplectic*, time-reversible approximate integrators [5,7]. More recently, an alternative symplectic thermostating scheme has been proposed based on a reformulation of Nosé dynamics in a separated form (with a constant mass matrix), incorporating an on-the-fly recovery of phase variables at fixed time steps through interpolation or reweighting [8].

In all of these methods, the production of canonically distributed phase-space trajectories requires the system to be sufficiently ergodic so that time and ensemble averages are equal within required accuracy. For the strongly coupled, many-particle systems generally encountered in molecular simulation, the dynamics is often sufficiently chaotic for this condition to be met. However, for certain important low-dimensional systems (such as the one-dimensional (1D) oscillators [9]) or for many-particle systems with weakly coupled low-dimensional subspaces (such as molecular systems with stiff intramolecular vibrations [10]), the addition of only two auxiliary Nosé variables is not enough to yield sufficiently ergodic phase-space trajectories. To remedy this, a number of methods have been proposed that either modify the coupling of the auxiliary variables in the Nosé-Hoover equations of state [11–14] or add additional auxiliary variables, as in the method of the Nosé-Hoover chains [15]. For a molecular system with periodic boundary conditions, the latter approach has proved to be the more generally useful one. All of these methods to enhance ergodicity, such as the

Nosé-Hoover approach from which they derive, are non-Hamiltonian in structure and cannot take advantage of symplectic integration schemes.

In this paper, we outline a general method for improving the ergodicity of the Nosé thermostat that is fully Hamiltonian in structure. The method is generated by the introduction of additional auxiliary variables to the Nosé-Poincaré thermostat, in much the same way as the Nosé-Hoover chains are generated from the Nosé-Hoover equations of motion. However, instead of specifically adopting a chainlike coupling for this extended Nosé-Poincaré Hamiltonian, we determine a general form for the coupling, from which an infinite variety of specific methods can be extracted. This general form is presented in Sec. III, following a background discussion of the mathematical formulation of Nosé based thermostats in Sec. II. In Sec. IV, specific examples of Generalized Nosé-Poincaré thermostats are introduced and analyzed with numerical experiments.

II. BACKGROUND: THE NOSÉ AND NOSÉ-POINCARÉ HAMILTONIANS

For a system of N particles in d dimensions, the original Nosé Hamiltonian is given by

$$\mathcal{H}_{\mathcal{N}}=\frac{\tilde{\mathbf{p}}^T\mathbf{M}^{-1}\tilde{\mathbf{p}}}{2s^2}+V(\mathbf{q})+\frac{\pi_s^2}{2Q_s}+gkT\ln s, \tag{1}$$

where $\mathbf{q}$ and $\tilde{\mathbf{p}}$ are the dN dimensional atomic position and conjugate Nosé momentum vectors, respectively, and the scalars s and π_s are auxiliary conjugate position and momentum variables. The Nosé dynamics controls the temperature of the system by rescaling time so that the real time t of the system is related to the Nosé time τ by $dt/d\tau=s$. In addition, the momentum $\mathbf{p}$ of the original system is related to the Nosé momentum by $\mathbf{p}=\tilde{\mathbf{p}}/s$.

The equations of motion for this system are

$$\frac{d\mathbf{q}}{d\tau}=\mathbf{M}^{-1}\mathbf{p}/s^2, \tag{2a}$$

$$\frac{d\tilde{\mathbf{p}}}{d\tau}=-\nabla V(\mathbf{q}), \tag{2b}$$

$$\frac{ds}{d\tau}=\frac{\pi_s}{Q_s}, \tag{2c}$$

$$\frac{d\pi_s}{d\tau}=\tilde{\mathbf{p}}^T\mathbf{M}^{-1}\tilde{\mathbf{p}}/s^3-gkT/s. \tag{2d}$$

The Nosé-Hoover equations of motion [15] are generated by transforming the time derivatives to real time, transforming to real momentum, and making the coordinate transformations $\eta=\ln s$ and $\xi=\dot{\eta}$. These coordinate and time transformations destroy the canonical Hamiltonian structure of the equations, although there is a conserved energy function.

As an alternative to Nosé-Hoover, the Nosé-Poincaré thermostat [5], a fully Hamiltonian real-time implementation of the Nosé thermostat, is obtained by applying a time transformation directly to the Nosé Hamiltonian as opposed to the equations of motion. The resulting transformed Hamiltonian is given by

$$H_{NP}=s[H_N-H_N(t=0)].$$

The Nosé-Poincaré Hamiltonian is nonseparable, since the kinetic energy contains the extended "position" variable s. The equations of motion for a general time-independent, nonseparable Hamiltonian can be written (for general positions Q and conjugate momenta P) as

$$\dot{Q}=G(P,Q),$$

$$\dot{P}=F(P,Q), \tag{3}$$

where $G(P,Q)=\partial\mathcal{H}/\partial P$ and $F(P,Q)=-\partial\mathcal{H}/\partial Q$. (For a separable Hamiltonian, G is only a function of P and F is only a function of Q.) For such a nonseparable system, standard symplectic splitting methods, such as the Verlet/leapfrog algorithm, are not directly applicable. However, symplectic methods specifically for nonseparable systems have been developed [3]. One simple example that is second order and time reversible is the generalized leapfrog algorithm (GLA)

$$P_{n+1/2}=P_n+hF(P_{n+1/2},Q_n)/2,$$

$$Q_{n+1}=Q_n+h[G(P_{n+1/2},Q_n)+G(P_{n+1/2},Q_{n+1})]/2,$$

$$P_{n+1}=P_{n+1/2}+hF(P_{n+1/2},Q_{n+1})/2, \tag{4}$$

where h is the time step and P_n and Q_n are the approximations to $P(t)$ and $Q(t)$ at $t=t_n=nh$. This method is a simple example of a class of symplectic integrators for nonseparable Hamiltonians [16–19]. Applying the GLA to the Nosé-Poincaré system gives a numerical method that is semiexplicit (requiring only one force evaluation per time step), symplectic, and time reversible.

The Nosé-Poincaré method is shown [5] to provide canonical sampling by an argument demonstrating that the microcanonical distribution function in the extended phase space,

$$\rho_{MC}(\mathbf{q},\mathbf{p},s,\pi_s;N,V,E_N)=\frac{1}{Z_{MC}}\delta(s[H_N(\mathbf{q},\mathbf{p},s,\pi_s)-E_N]) \tag{5}$$

(where Z_{MC} is the microcanonical partition function obtained by integrating ρ_{MC} over the extended phase space) generates a canonical distribution in the reduced phase space. The proof relies on simply performing the integrations with respect to the auxiliary variables.

III. A GENERALIZED EXTENDED NOSÉ THERMOSTAT

In this section, we show that the Nosé approach (and its corresponding real-time version—Nosé-Poincaré) is only the simplest realization of a vast range of generalized thermostating Hamiltonians. In particular, we show below that ca-

nonical sampling can be achieved as well if the Nosé Hamiltonian is coupled to an auxiliary system (with position variables $\{\sigma_i\}$ and conjugate momenta $\{\pi_i\}$) to generate a generalized Nosé Hamiltonian

$$H_{GN}=H(\mathbf{q},\tilde{\mathbf{p}}/s)+gkT\ln s+f(\pi_s,\{\sigma_i,\pi_i\}), \tag{6}$$

where H is the Hamiltonian for the original system to be thermostated, s and π_s are the usual Nosé thermostat variables, and f is a continuous function that must be chosen so that it is bounded below and so that $\exp(-\beta f)$ is in L_1 on its domain, i.e., so that its absolute integral is finite. The corresponding real-time generalized Nosé-Poincaré Hamiltonian is then

$$H_{GNP}=s[H_{GN}-H_{GN}(t=0)]. \tag{7}$$

The proof that this generalized Nosé-Poincaré generates a canonical distribution (assuming ergodicity) follows closely that for the standard Nosé-Poincaré approach [5] and is given here for completeness. The statistical distribution for the reduced set of variables, $\mathcal{P}(\mathbf{p},\mathbf{q})$, is given by an integral over the extended variable distribution $\mathcal{P}_{ext}(\mathbf{p},\mathbf{q},s,\mathbf{\Lambda})$ [where $\mathbf{\Lambda}$ denotes the vector of auxiliary variables $(\pi_s,\{\sigma_i\},\{\pi_i\})$]:

$$d\mathbf{q}d\mathbf{p}\mathcal{P}(\mathbf{p},\mathbf{q})=\int d\mathbf{q}d\tilde{\mathbf{p}}dsd\mathbf{\Lambda}\mathcal{P}_{ext}(\mathbf{p},\mathbf{q},s,\mathbf{\Lambda}), \tag{8}$$

where the integral is over the auxiliary variables s and $\mathbf{\Lambda}$. Assuming that the dynamics is ergodic,

$$d\mathbf{q}d\mathbf{p}\mathcal{P}(\mathbf{p},\mathbf{q})=\frac{1}{Z_{GN}N!h^{N_f}}\int ds\int d\mathbf{\Lambda}d\tilde{\mathbf{p}}d\mathbf{q}\,\delta(s[H(\mathbf{p}/s,\mathbf{q})+gkT\ln s+f(\mathbf{\Lambda})-H_{GN}(0)]), \tag{9}$$

where Z_{GNP} represents the partition function for the generalized Nosé-Poincaré Hamiltonian and N_f is the number of degrees of freedom in the thermostated system. Changing variables to real momenta $\mathbf{p}=\tilde{\mathbf{p}}/s$ gives

$$d\mathbf{q}d\mathbf{p}\mathcal{P}(\mathbf{p},\mathbf{q})=\frac{d\mathbf{p}d\mathbf{q}}{Z_{GN}N!h^{N_f}}\int dsd\mathbf{\Lambda}s^{N_f}\delta(s[H(\mathbf{p},\mathbf{q})+gkT\ln s+f(\mathbf{\Lambda})-H_{GN}(0)]). \tag{10}$$

For a function $\phi(s)$ with a single pole at $s=s_0$, we have

$$\delta(\phi(s))=\frac{\delta(s-s_0)}{|\phi'(s_0)|},$$

which, for our case, gives

$$d\mathbf{q}d\mathbf{p}\mathcal{P}(\mathbf{p},\mathbf{q})=\frac{d\mathbf{p}d\mathbf{q}}{Z_{GN}N!h^{N_f}}\int ds\int d\mathbf{\Lambda}\frac{s^{N_f}}{gkT}\times\delta\left(s-\exp\left\{-\frac{1}{gkT}[H(\mathbf{p},\mathbf{q})+f(\mathbf{\Lambda})-H_{GN}(0)]\right\}\right). \tag{11}$$

Integration over s yields

$$d\mathbf{q}d\mathbf{p}\mathcal{P}(\mathbf{p},\mathbf{q})=\frac{d\mathbf{q}d\mathbf{p}}{gkTZ_{GN}N!h^{N_f}}\int d\mathbf{\Lambda}\exp\left\{-\frac{N_f}{gkT}[H(\mathbf{p},\mathbf{q})+f(\mathbf{\Lambda})-H_{GN}(0)]\right\}. \tag{12}$$

Setting $g=N_f$ and integrating over the remaining auxiliary variables $\mathbf{\Lambda}$ give

$$\mathcal{P}(\mathbf{p},\mathbf{q})=\frac{C}{Z_{GN}N!h^{N_f}}\exp[-\beta H(\mathbf{p},\mathbf{q})], \tag{13}$$

where $\beta=(kT)^{-1}$ and we have assumed certain properties of the function $f(\mathbf{\Lambda})$ to ensure that the integration converges, namely, (1) f is bounded below, (2) $\exp(-\beta f)\in L_1$. Applying the same procedure to Z_{GN} and canceling constants gives

$$\mathcal{P}(\mathbf{p},\mathbf{q})=\frac{1}{ZN!h^{N_f}}\exp\{-\beta[H(\mathbf{p},\mathbf{q})]\}, \tag{14}$$

which is the usual canonical distribution, with Z being the standard canonical partition function:

$$Z=\frac{1}{N!h^{N_f}}\int d\mathbf{p}\int d\mathbf{q}\exp\{-\beta[H(\mathbf{p},\mathbf{q})]\}. \tag{15}$$

(It should be noted that in the original Nosé-Poincaré paper [5], a method for Nosé-Poincaré chains was outlined; however, this method violates the conditions on f given above and is invalid.)

A useful subclass of generalized Nosé Hamiltonians can be generated by viewing the standard Nosé Hamiltonian as the "system" and the auxiliary variable $\{\sigma_i,\pi_i\}$ as a "bath" giving

$$H_{GN}=H_N(\tilde{\mathbf{p}},\mathbf{q},s,\pi_s)+H_{\text{bath}}(\{\sigma_i,\pi_i\})+H_{\text{int}}(\pi_s,\{\sigma_i,\pi_i\}), \tag{16}$$

where H_N is the usual Nosé Hamiltonian and the system-bath interaction Hamiltonian H_{int} has no dependence on s to preserve the canonical distribution, but is otherwise arbitrary (within the constraints on f outlined above). *This gives us the result that a given Hamiltonian system can be thermostated by coupling it to any other system, including a copy of itself.*

For such a broad class of generalized Hamiltonians, it is not possible to give a general numerical discretization scheme that is optimal for all members of the class, but for any given specific case, efficient schemes can be devised. In the following section, we give two specific examples of generalized Nosé-Poincaré systems and outline efficient, symplectic numerical integration algorithms for each.

IV. ALGORITHMS AND NUMERICAL EXPERIMENTS

In this section, two examples of generalized Nosé-Poincaré thermostats are presented along with appropriate symplectic numerical discretization schemes. In addition, numerical experiments are performed to show that these methods can successfully thermostat a 1D harmonic oscillator. Note that these are merely intended as representative examples of the infinite set of possible generalized thermostats and are in no sense being touted as optimal.

A. Example 1: "Vertex" coupling to independent harmonic oscillators

Consider the following specific generalized Nosé Hamiltonian:

$$\mathcal{H}_{\mathcal{GN}}=\frac{\tilde{\mathbf{p}}^T\mathbf{M}^{-1}\tilde{\mathbf{p}}}{2s^2}+V(\mathbf{q})+gkT\ln s+\frac{\left(1+\sum\ \sigma_i^2\right)\pi_s^2}{2Q_s}+\sum_i\frac{\sigma_i^2}{2}+\sum_{i=1,m}\frac{\pi_i^2}{2Q_i}. \tag{17}$$

We refer to this model as a ''vertex'' coupling as the σ_i are only coupled to the other variables through π_s (a common vertex). The generalized Nosé-Poincaré Hamiltonian for this system is generated in the usual way,

$$H_{GNP}=s[H_{GN}-H_{GN}(t=0)]. \tag{18}$$

The equations of motion for this example generalized Nosé-Poincaré system are

$$\dot{\tilde{\mathbf{p}}}=-s\nabla V(\mathbf{q}), \tag{19a}$$

$$\dot{\mathbf{q}}=\mathbf{M}^{-1}\tilde{\mathbf{p}}/s, \tag{19b}$$

$$\dot{s}=\frac{s\left(1+\sum\ \sigma_i^2\right)\pi_s}{Q_s}, \tag{19c}$$

$$\dot{\pi}_s=\tilde{\mathbf{p}}^T\mathbf{M}^{-1}\tilde{\mathbf{p}}/s^2-gkT-[H_{GN}-H_{GN}(t=0)], \tag{19d}$$

$$\dot{\sigma}_i=\frac{s\pi_i}{Q_i}, \tag{19e}$$

$$\dot{\pi}_i=-s(1+\pi_s^2/Q_s)\sigma_i. \tag{19f}$$

To generate a symplectic integration scheme, often the best approach is to use a splitting method in which the Hamiltonian is written as the sum of simpler Hamiltonians for which the equations of motion can be integrated either exactly or with known simple symplectic schemes [3]. The overall discretization scheme is then given as the concatenation of those for the subproblems. For this vertex generalized Nosé-Poincaré, the following splitting can be used:

$$H_1=-s\left[\frac{\left(1+\sum\ \sigma_i^2\right)\pi_s^2}{2Q_s}+\frac{1}{2}\sum_i\ \sigma_i^2+gkT\ln s\right], \tag{20}$$

$$H_2=s\left[\frac{\tilde{\mathbf{p}}^T\mathbf{M}^{-1}\tilde{\mathbf{p}}}{2s^2}+\sum\frac{\pi_i^2}{2Q_i}\right], \tag{21}$$

$$H_3=s[V(q)-H_{GNP}(t=0)]. \tag{22}$$

This splitting is similar to one proposed by Nosé for the original Nosé-Poincaré method [7]. The numerical method is then generated by the concatenation

$$\phi_H(t)=\phi_{H_1}(t/2)\,\phi_{H_2}(t/2)\,\phi_{H_3}(t)\,\phi_{H_2}(t/2)\,\phi_{H_1}(t/2)+O(t^3), \tag{23}$$

where $\phi_H(t)$ is the solution map that advances a phase-space point forward in time by t under the dynamics defined by the Hamiltonian H. The solution maps for H_2 and H_3 can be performed exactly and that for H_1 can be approximated using the GLA discussed in Sec. II to yield a second-order method that is both time reversible and symplectic.

B. Example 2: Coupling to a "realistic" system, the three-soft-particle bath

A standard example of a system that is provably ergodic is the three-ball billiard system consisting of three hard-sphere particles moving in a box with hard boundaries [20]. While we could, in principle, develop numerical schemes for handling a hard-sphere bath, using the technique described in Ref. [21], this would be quite complicated. Instead, for the purposes of this demonstration, we use a simplified bath consisting of three soft repulsive spheres constrained to a soft cubic box. Using the system-bath notation in Eq. (16), the bath and interaction Hamiltonians for this system are given by

$$H_{\text{bath}}=\sum_{i=1}^3\frac{|\boldsymbol{\pi}_i|^2}{2Q_i}+\sum_{i=1}^3\left[\left(\frac{\sigma_{i,x}}{l}\right)^{12}+\left(\frac{\sigma_{i,y}}{l}\right)^{12}+\left(\frac{\sigma_{i,z}}{l}\right)^{12}\right]+\sum_i\sum_{j>i}|\boldsymbol{\sigma}_i-\boldsymbol{\sigma}_j|^{-12} \tag{24}$$

and

$$H_{\text{int}}=\left(\sum_{i=1}^3|\boldsymbol{\sigma}_i|^2\right)\frac{|\boldsymbol{\pi}_s|^2}{2Q_s}. \tag{25}$$

Here the bath positions and momenta $\boldsymbol{\sigma}_i$ and $\boldsymbol{\pi}_i$ are vectors in $\mathcal{R}^3$ and the second term in Eq. (24) defines a soft cubic box of side length l. The Nosé-Poincaré equations for this system can be integrated using a similar Hamiltonian splitting to that used in the vertex coupling,

$$H_1 = s\left\{ gkT\ln s + \left(\sum_{i=1,3} |\boldsymbol{\sigma}_i|^2 \right)\left(\frac{\pi_s^2}{2Q_s} \right) + \sum_{i=1}^{3} \left[\left(\frac{\sigma_{i,x}}{l} \right)^{12} + \left(\frac{\sigma_{i,y}}{l} \right)^{12} + \left(\frac{\sigma_{i,z}}{l} \right)^{12} \right] + \sum_i \sum_{j>i} |\boldsymbol{\sigma}_i - \boldsymbol{\sigma}_j|^{-12} \right\},$$

$$H_2 = s\left[\frac{\mathbf{p}^T \mathbf{M}^{-1} \mathbf{p}}{2s^2} + \sum_{i=1}^{3} \frac{|\boldsymbol{\pi}_i|^2}{2Q_i} \right],$$

$$H_3 = s[V(\mathbf{q}) - H_{GN}(t=0)]. \tag{26}$$

The dynamics for H_2 and H_3 can be integrated exactly and that for H_1 can be integrated using the GLA discussed in Sec. II.

C. Numerical experiments

We apply the two generalized Nosé-Poincaré Hamiltonians above to the problem of thermostating a 1D harmonic oscillator. This system exhibits quite severe deviations from ergodicity for the unaugmented Nosé thermostats [15], which is the main reason for the difficulty encountered in thermostating molecular systems with stiff bonds that are weakly coupled to the rest of the system [10]. The unthermostated Hamiltonian for this system is

$$H(p,q) = \frac{p^2}{2} + \frac{q^2}{2},$$

where we have assumed unit mass and angular frequency.

To test the sampling, we have performed molecular-dynamics simulations at $kT=1.0$ on this model using both the vertex coupling (with $Q_s=1.0$ and 6 auxiliary variables with arbitrarily chosen masses Q_i equal to 0.7, 1.25, 5.2, 10.35, 19, and 29.5) and the three-ball coupling (with $Q_s=7.0$, $l=2.5$, and all sphere masses set to 1.0). In Fig. 1, the results for the distribution of q for both couplings in the runs of 2×10^6 steps with a time step $h=0.01$ are shown. The solid line in Fig. 1 shows, for comparison, the exact canonical distribution for this system at the target temperature and the dotted line shows the results for the standard Nosé-Poincaré method with $Q_s=1.0$ (with identical time step and run length). Under these conditions, both extended Nosé-Poincaré methods are seen to adequately generate a canonical distribution for the harmonic oscillator position variable. Similar agreement is obtained for the momentum distribution. In all cases, the energy error was less than 1×10^{-4} with no discernible energy drift.

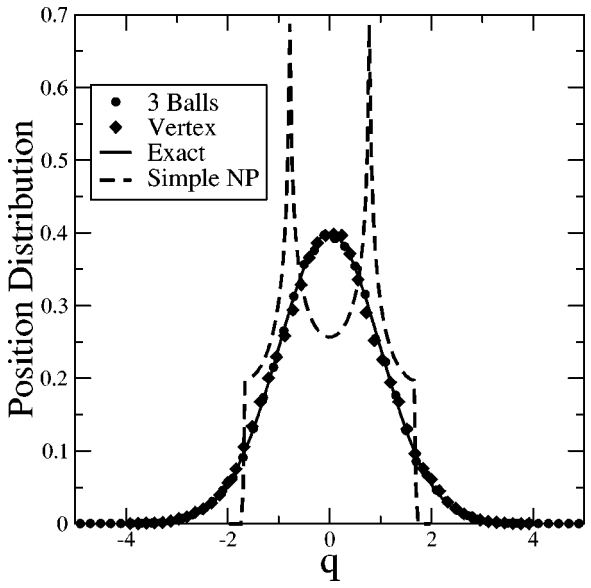

FIG. 1. The probability distribution for the position q of a harmonic oscillator thermostated at $kT=1.0$ by the generalized Nosé-Poincaré vertex (diamonds) and three-sphere (circles) couplings discussed in Sec. IV. Specific parameters used for each simulation are given in the text. For comparison, the exact canonical distribution expected is shown as a solid line and the dotted line represents a simulation using the original Nosé-Poincaré thermostat with a thermostat mass of unity.

V. CONCLUSIONS

We have demonstrated that the Nosé [1,2] and Nosé-Poincaré [5] methods for constant-temperature molecular-dynamics simulation can be substantially generalized by the addition of auxiliary variables to encompass an infinite variety of Hamiltonian thermostats. Such thermostats can be used to enhance ergodicity in systems, such as the 1D harmonic oscillator [9] or certain molecular systems [10], for which the standard Nosé-Hoover [9] and Nosé-Poincaré methods fail to reproduce converged canonical distributions. The addition of additional variables to an extended Hamiltonian system is much in the spirit of previous work to improve the convergence of the non-Hamiltonian Nosé-Hoover thermostat, namely, through the use of the Nosé-Hoover chains [15] or Gaussian thermostating [14], but the methods described in this work are far more general and are fully Hamiltonian in form, which allows for the use of symplectic integration schemes, which have been shown to have superior stability in long simulations [3].

In particular, we demonstrate the remarkable result that, within the generalized Nosé formalism outlined herein, any Hamiltonian system can be thermostated with any other, including a copy of itself. This gives one an enormous flexibility in choosing the form of the thermostating bath. For example, one could use as the thermostating bath system a collection of coupled oscillators with natural frequencies that mimic those in the system to be thermostated allowing for more efficient energy transfer from system to bath. In this multiresonant Nosé approach, the bath frequencies and couplings could be tuned for optimal performance. In another approach, one could use as the thermostating system a subset of the full system; for example, one could thermostat a system of biomolecules in solution with a small sample of water at the desired temperature. It is clear that further study is needed to understand how one constructs an optimal thermostating bath for a given system. The generalized Nosé approach provides a useful general framework within which such investigations can be undertaken in a systematic way.

ACKNOWLEDGMENTS

The authors wish to thank Chris Sweet for valuable computational assistance. B.B.L. gratefully acknowledges support from the National Science Foundation under Grant No. CHE-9970903 and the hospitality of the Center for Mathematical Modelling at the University of Leicester, where much of this work was undertaken. In addition, B.J.L. acknowledges the U.K. Engineering and Physical Sciences Research Council Grant No. GR/R03259/01.

[1] S. Nosé, Mol. Phys. **52**, 255 (1984).
[2] S. Nosé, J. Chem. Phys. **81**, 511 (1984).
[3] J.M. Sanz-Serna and M.P. Calvo, *Numerical Hamiltonian Problems* (Chapman and Hall, New York, 1995).
[4] G.J. Martyna, M.E. Tuckerman, D.J. Tobias, and M.L. Klein, Mol. Phys. **87**, 1117 (1996).
[5] S.D. Bond, B.J. Leimkuhler, and B.B. Laird, J. Comput. Phys. **151**, 114 (1999).
[6] C.P. Dettmann and G.P. Morriss, Phys. Rev. E **54**, 2495 (1996).
[7] S. Nosé, J. Phys. Soc. Jpn. **70**, 75 (2001).
[8] B.J. Leimkuhler, Comput. Phys. Commun. **148**, 206 (2002).
[9] W.G. Hoover, Phys. Rev. A **31**, 1695 (1985).
[10] S. Toxværd, Ber. Bunsenges. Phys. Chem. **94**, 274 (1990).
[11] I.P. Hamilton, Phys. Rev. A **42**, 7467 (1990).
[12] D. Kusnezov, A. Bulgac, and W. Bauer, Ann. Phys. (San Diego) **204**, 155 (1990).
[13] R. G Winkler, Phys. Rev. A **45**, 2250 (1992).
[14] Y. Liu and M.E. Tuckerman, J. Chem. Phys. **112**, 1685 (2000).
[15] G.J. Martyna, M.L. Klein, and M. Tuckermann, J. Chem. Phys. **97**, 2635 (1992).
[16] J.M. Sanz-Serna, BIT **28**, 877 (1991).
[17] F. Lasagni, Z. Angew. Math. Phys. **39**, 952 (1988).
[18] Y.B. Suris, USSR Comput. Math. Math. Phys. **29**, 138 (1989).
[19] J.M. Sanz-Serna, Acta Numer. **1**, 243 (1991).
[20] L. Bunimovich, C. Liverani, A. Pellegrinotti, and Yu. Sukhov, Commun. Math. Phys. **146**, 357 (1992).
[21] Y.A. Hounonougbo, B.B. Laird, and B.J. Leimkuhler, Mol. Phys. **98**, 309 (1999).